

Electronic Supplementary Information (ESI[†])

Structural Modification of Nickel Tetra(thiocyano)corroles during Electrochemical Water Oxidation

Panisha Nayak,^a Ajit Kumar Singh,^b Manisha Nayak,^a Subhajit Kar,^a Kasturi Sahu,^a Kiran Meena,^a Dinesh Topwal,^c Arindam Indra^{*,b} and Sanjib Kar^{*,a}

^a*School of Chemical Sciences, National Institute of Science Education and Research (NISER), Bhubaneswar – 752050, India, and Homi Bhabha National Institute, Training School Complex, Anushakti Nagar, Mumbai, 400 094, India. E-mail: sanjib@niser.ac.in*

^b*Department of Chemistry, IIT(BHU), Varanasi, Uttar Pradesh-221005, India. E-mail: arindam.chy@iitbhu.ac.in*

^c*Institute of Physics, Bhubaneswar 751005, India and Homi Bhabha National Institute, Training School Complex, Anushakti Nagar, Mumbai, 400 094, India.*

Appendix 1: Experimental Details of Electrochemical Measurement**Appendix 2:** HOMA calculations**Appendix 3:** Determination of the number of active sites of the Ni(O)(OH)/Ni-corrole with respect to the different activation cycles.**Table S1** Crystallographic data for **1**.**Table S2** UV-Vis. and electrochemical data for **1** and **2**.**Table S3** Comparison of the number of active sites of the Ni(O)(OH)/Ni-corrole with respect to the different activation cycles.**Fig. S1** Visualization of atomic displacement parameters (ADPs) in the X-ray crystallographic depiction of **1**.**Fig. S2** Electronic absorption spectrum of **1** in acetonitrile at 298 K.**Fig. S3** Electronic absorption spectrum of **2** in acetonitrile at 298 K.**Fig. S4** Evolution of the electronic absorption spectra of **2** in the presence of excess triethylamine and trifluoroacetic acid in CH₃CN.**Fig. S5** ESI-MS spectrum of 2,3,17,18-Tetrathiocyanato-[5,10,15-tris(4-cyanophenyl)corrolato] nickel(II), **1** in CH₃CN shows the (a) measured spectrum with isotopic distribution pattern (experimental) and (b) isotopic distribution pattern (simulated).**Fig. S6** ESI-MS spectrum of 2,3,17,18-Tetrathiocyanato-[5,15-bis(4-cyanophenyl)-10-(4-bromophenyl)-corrolato] nickel(II), **2** in CH₃CN shows the (a) measured spectrum with isotopic distribution pattern (experimental) and (b) isotopic distribution pattern (simulated).**Fig. S7** ¹H-NMR spectrum of **1** in CD₃CN solution.**Fig. S8** ¹³C {¹H}-NMR spectrum of **1** in CD₃CN solution.**Fig. S9** ¹H-NMR spectrum of **2** in CD₃CN solution.**Fig. S10** ¹³C {¹H}-NMR spectrum of **2** in CD₃CN solution.**Fig. S11** LSV profiles of Ni(O)(OH)/Ni-corrole (active catalyst after 100 CV cycles), Ni(O)OH, Ni-corrole, and another molecular complex Ni(dmgH)₂ and bare CC in a 1.0 M aqueous KOH solution (scan rate 2 mV s⁻¹).

- Fig. S12** LSV profiles of the Ni(O)(OH)/Ni-corrole@CC with Pt as counter electrode (blue) and Ni(O)(OH)/Ni-corrole@CC with respect to glassy carbon (green) as counter electrode in 1.0 M aqueous KOH solution.
- Fig. S13** Electrochemical activation of Ni(O)(OH)/Ni-corrole via the addition of Fe³⁺ to the electrolyte solution, as depicted by a CV cycle.
- Fig. S14** Potential vs. current density plots showing the oxidation peak used for the area integration curve.
- Fig. S15** PXRD of the Ni(O)(OH)/Ni-corrole after 3 CV cycles, 30 CV cycles, and 100 CV cycles.⁵
- Fig. S16** Raman spectra of the Ni(O)(OH)/Ni-corrole after 100 cycles.⁶
- Fig. S17** UV-visible spectra showed the peaks corresponding to the Ni(O)(OH)/Ni-corrole after 30 CV cycles and 100 CV cycles activation.⁷
- Fig. S18** (a-c) The SEM and EDX studies of Ni(O)(OH)/Ni-corrole after the different CV cycle activations showed a change in the morphological feature. (e-g) The EDX data of the catalyst after 3 cycles, 30 cycles, and 100 cycles of CV activation showed that Ni, C, N, O, and S but with a varying amount.
- Fig. S19** The chronoamperometric study of Ni(O)(OH)/Ni-corrole demonstrates the stability of the catalyst for 6 hours.
- Fig. S20** The plausible mechanism for the formation of Ni(O)OH from the Ni-corrole complex by the anodic activation in the alkaline medium.

Appendix 1: Experimental Details of Electrochemical Measurement

Activation of carbon cloth

1 cm x 2 cm of carbon cloth was first washed with acetone twice under ultrasonication, then five times with water. Clean carbon cloth was dried at 50 °C for 12 h and treated with nitric acid for 4 h at 100°C. The activated carbon cloth was dried in an air oven at 50° C and used for catalyst deposition.¹

Deposition of molecular catalyst on the carbon cloth

4 mg of molecular catalysts were dissolved in 100 mL of ethanol by using ultrasonication for 3 minutes, then 10 microliters of an ethanolic 0.05 wt% Nafion solution was added, then again sonicated for 2 minutes. The liquid was then dropped and cast onto activated carbon cloth (CC).

Electrochemical measurement

OER and HER experiments were conducted in a 1.0 M aqueous KOH solution in a single compartment having a three-electrode electrochemical cell. We used molecular complex@CC as the working electrode, a Pt wire counter electrode, and an Ag/AgCl as a reference electrode. The equation $E_{(RHE)} = E_{(Ag/AgCl)} + 0.097 \text{ V} + (0.059 \text{ pH}) \text{ V}$ was used to convert the potentials provided above to the RHE.² A constant potential was used in a 1.0 M KOH solution to conduct a chronoamperometric experiment at 1.60 V vs. RHE. All CV and LSV have been 75% iR corrected. To understand this, the electrochemical activation of the molecular catalyst was performed to reach a constant current density. After that, 2 mg of $FeCl_3$ was added to the electrolyte solution, and the CV cycle was continued.³

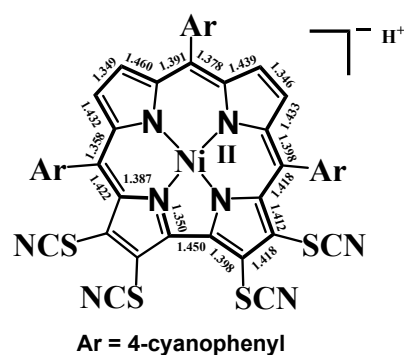
1. A. Indra, U. Paik and T. Song, *Angew. Chem. Int. Ed.*, 2018, **57**, 1241-1245.
2. B. B. Yu, Y. W. Hua, Q. Huang, S. Y. Ye, H. D. Zhang, Z. Yan, R. W. Li, J. Wu, Y. Meng and X. Cao, *CrystEngComm*, 2021, **23**, 4700-4707.
3. S. K. Pal, B. Singh, J. K. Yadav, C. L. Yadav, M. G. B. Drew, N. Singh, A. Indra and K. Kumar, *Dalton Trans.*, 2022, **51**, 13003–13014.

Appendix 2: HOMA calculations

The HOMA values¹ of 2,3,17,18-tetra(thiocyano)-[5,10,15-tris(4-cyanophenyl)corrolato]nickel(II) (1) and [5,10,15-tris(pentafluorophenyl)corrolato]nickel(II)² were calculated using the C–C and C–N bond lengths obtained from their X-ray crystallographic structures, according to the following equations:³

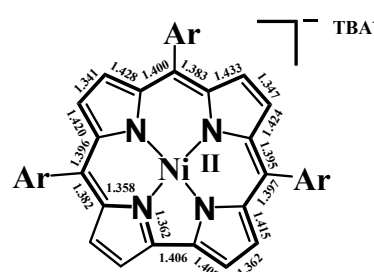
$$\text{HOMA} = 1 - \frac{1}{n} \left\{ \alpha_{CC} \sum (R_{opt} - R_i)_{CC}^2 + \alpha_{CN} \sum (R_{opt} - R_i)_{CN}^2 \right\}$$

where n = number of bonds taken into summation, α = empirical constant, R_{opt} = optimal bond length and R_i = bond length of i^{th} bond.



2,3,17,18-tetra(thiocyano)-[5,10,15-tris(4-cyanophenyl)corrolato] nickel(II), 1

HOMA=0.64



Tris(pentafluorophenyl)corrolato] nickel(II)²

HOMA=0.81

Selected bond distances and calculated HOMA values¹ for single-crystal structures of 2,3,17,18-tetra(thiocyano)-[5,10,15-tris(4-cyanophenyl)corrolato] nickel(II), **1**, and [5,10,15-tris(pentafluorophenyl)corrolato]nickel(II).² The bonds used for HOMA calculations are indicated in bold lines.

References:

- (a) J. Kruszewski and T. M. Krygowski, *Tetrahedron Lett.* 1972, 13, 3839– 3842; (b) T. M. Krygowski, H. Szatyłowicz, O. A. Stasyuk, J. Dominikowska, M. Palusiak, *Chem. Rev.* 2014, 114, 6383– 6422; (c) C. P. Frizzo and M. A. P. Martins, *Struct. Chem.* 2012, 23, 375– 380.
- Q. C. Chen, S. Fite, N. Fridman, B. Tumanskii, A. Mahammed and Z. Gross, *ACS Catal.*, 2022, **12**, 4310-4317.
- (a) C. A. Hunter, J. K. M. Sanders, *J. Am Chem. Soc.*, 1990, **112**, 5525–5534; (b) R. Nozawa, H. Tanaka, W.-Y. Cha, Y. Hong, I. Hisaki, S. Shimizu, J.-Y. Shin, T. Kowalczyk, S. Irle, D. Kim, *Nat. Commun.* **2016**, **7**, 13620.

Table S1 Crystallographic data for **1**.

compound code	1
chemical formula	C ₈₈ H _{30.40} N ₂₂ Ni ₂ S ₈
formula mass	1769.64
crystal system	Triclinic
crystal size (mm)	0.13×0.12×0.10
space group	<i>P-1</i>
Radiation	Mo <i>K</i> α
<i>a</i> (Å)	13.5052 (3)
<i>b</i> (Å)	16.0286 (4)
<i>c</i> (Å)	25.3258 (7)
<i>α</i> (deg)	97.682 (2)
<i>β</i> (deg)	102.718 (2)
<i>γ</i> (deg)	90.036 (2)
<i>V</i> (Å ³)	5297.2 (2)
<i>Z</i>	2
<i>T</i> (K)	100.01(11)
<i>D</i> _{calcd} (g cm ⁻³)	1.109
measured reflections	46982
<i>e</i> data (<i>R</i> _{int})	11888 (0.0614)
parameters	1081
restraints	1004
<i>μ</i> (mm ⁻¹)	0.561
2 <i>θ</i> range (deg)	6.43 – 50.00
<i>R</i> 1 (<i>I</i> > 2σ(<i>I</i>))	0.0784
WR2 (all data)	0.2106
S (GooF) all data	1.025
Δ <i>ρ</i> _{max} , Δ <i>ρ</i> _{min} (e Å ⁻³)	0.884, -0.559

Table S2 UV-Vis. and electrochemical data for **1** and **2**.

Compound	UV-vis. Data ^a $\lambda_{\text{max}} / \text{nm} (\epsilon / \text{M}^{-1}\text{cm}^{-1})$	Electrochemical data ^{a,b}	
		Oxidation $E^0, \text{V} (\Delta E_{\text{p}}, \text{mV})$	Reduction $E^0, \text{V} (\Delta E_{\text{p}}, \text{mV})$
1	401 (70700), 418 (82700), 563 (35300), 592 (69000), 608 (92700)	+0.71 (80), +1.12 (80)	1.29
2	401 (71700), 418 (85500), 564 (31700), 592 (60600), 611 (87400).	+0.72 (80), +1.14 (80)	1.35

^a In acetonitrile.

^b The potentials are *versus* Ag/AgCl.

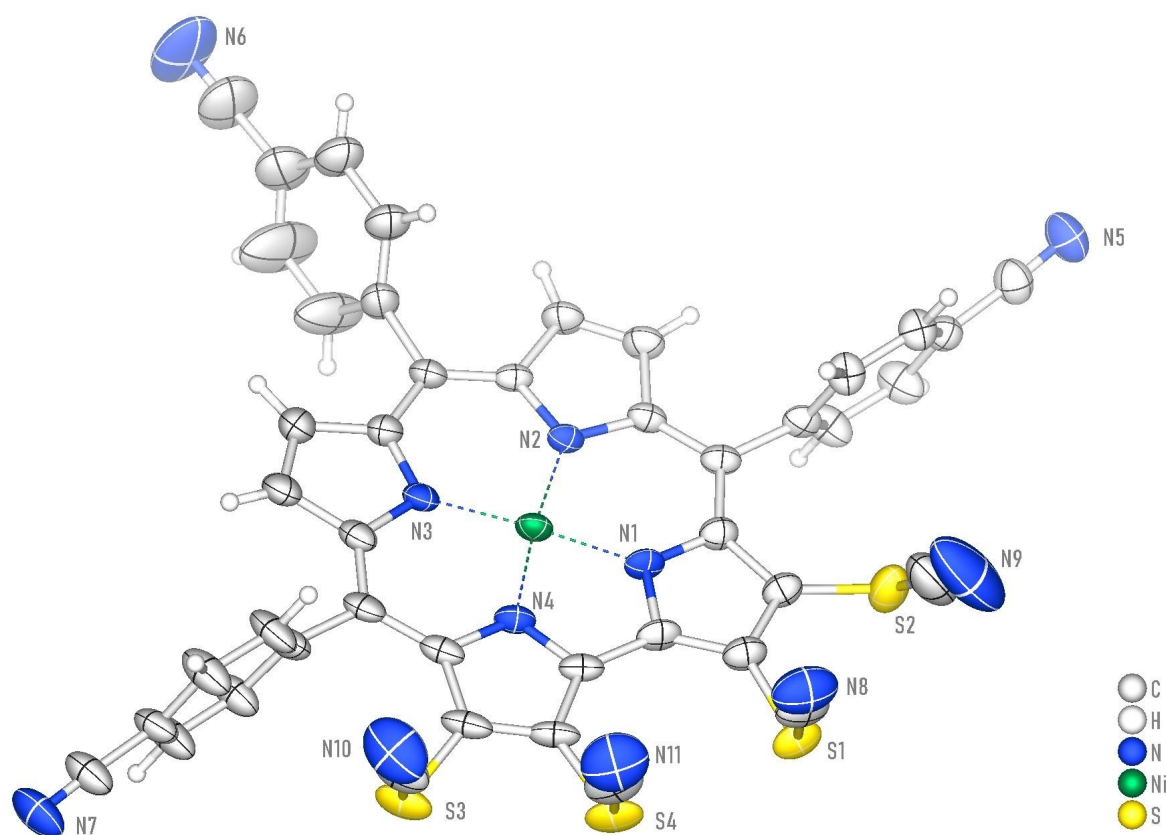


Fig. S1 Visualization of atomic displacement parameters (ADPs) in the X-ray crystallographic depiction of **1**.

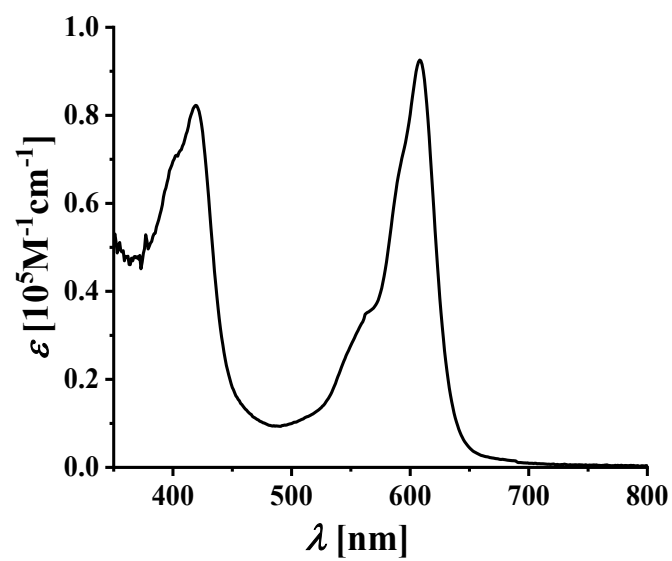


Fig. S2 Electronic absorption spectrum of **1** in acetonitrile at 298 K.

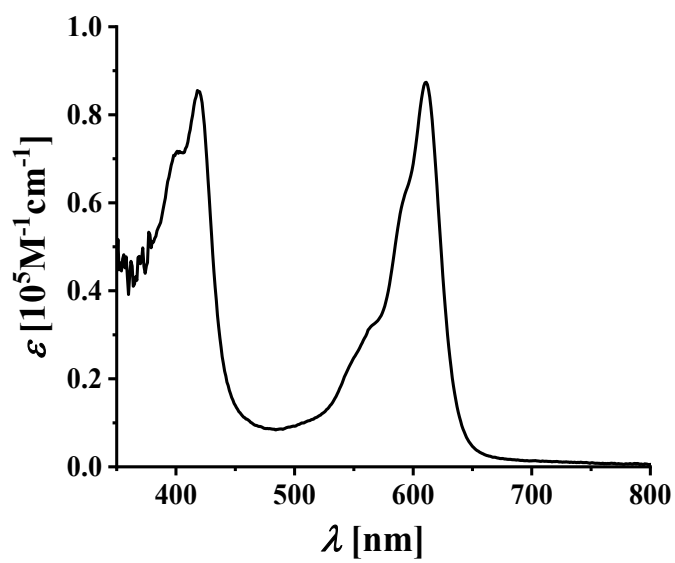


Fig. S3 Electronic absorption spectrum of **2** in acetonitrile at 298 K.

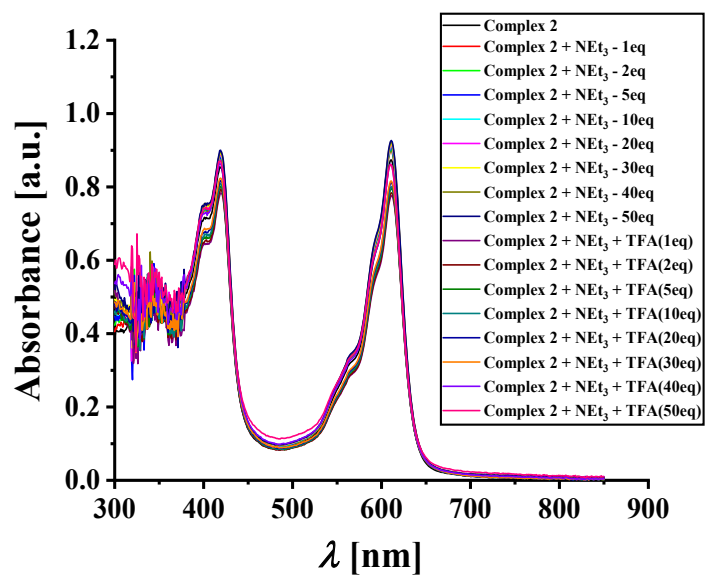


Fig. S4 Evolution of the electronic absorption spectra of **2** in the presence of excess triethylamine and trifluoroacetic acid in CH₃CN.

SK_Ni TCCSCN

05-Mar-2024
15:02:19

SK_05032024_1 44 (0.761) Cm (43:50)

XEVO-G2XSQTOF#NotSet

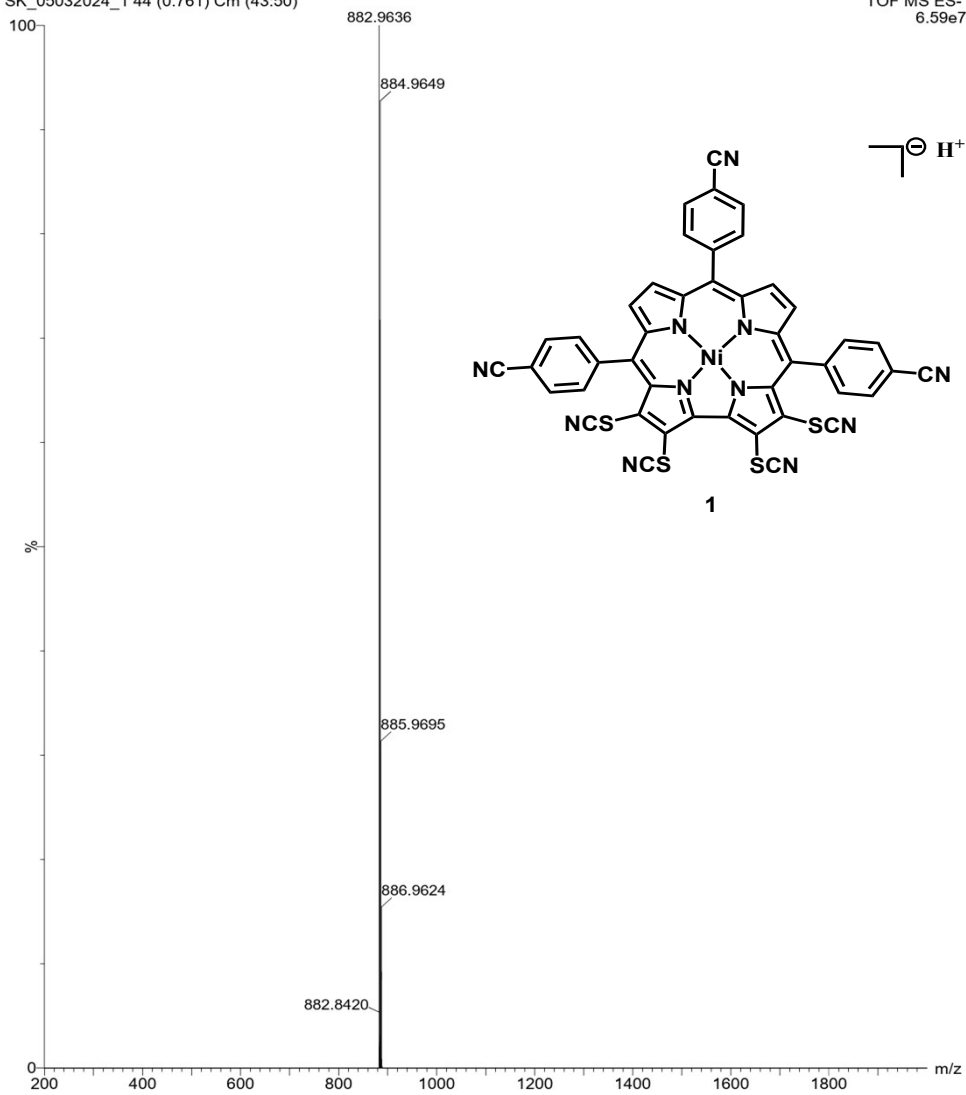
TOF MS ES-
6.59e7

Fig. S5 (a) ESI-MS spectrum of 2,3,17,18-Tetrathiocyanato-[5,10,15-tris(4-cyanophenyl)corrolato] nickel(II), **1** in CH₃CN shows the measured spectrum (experimental).

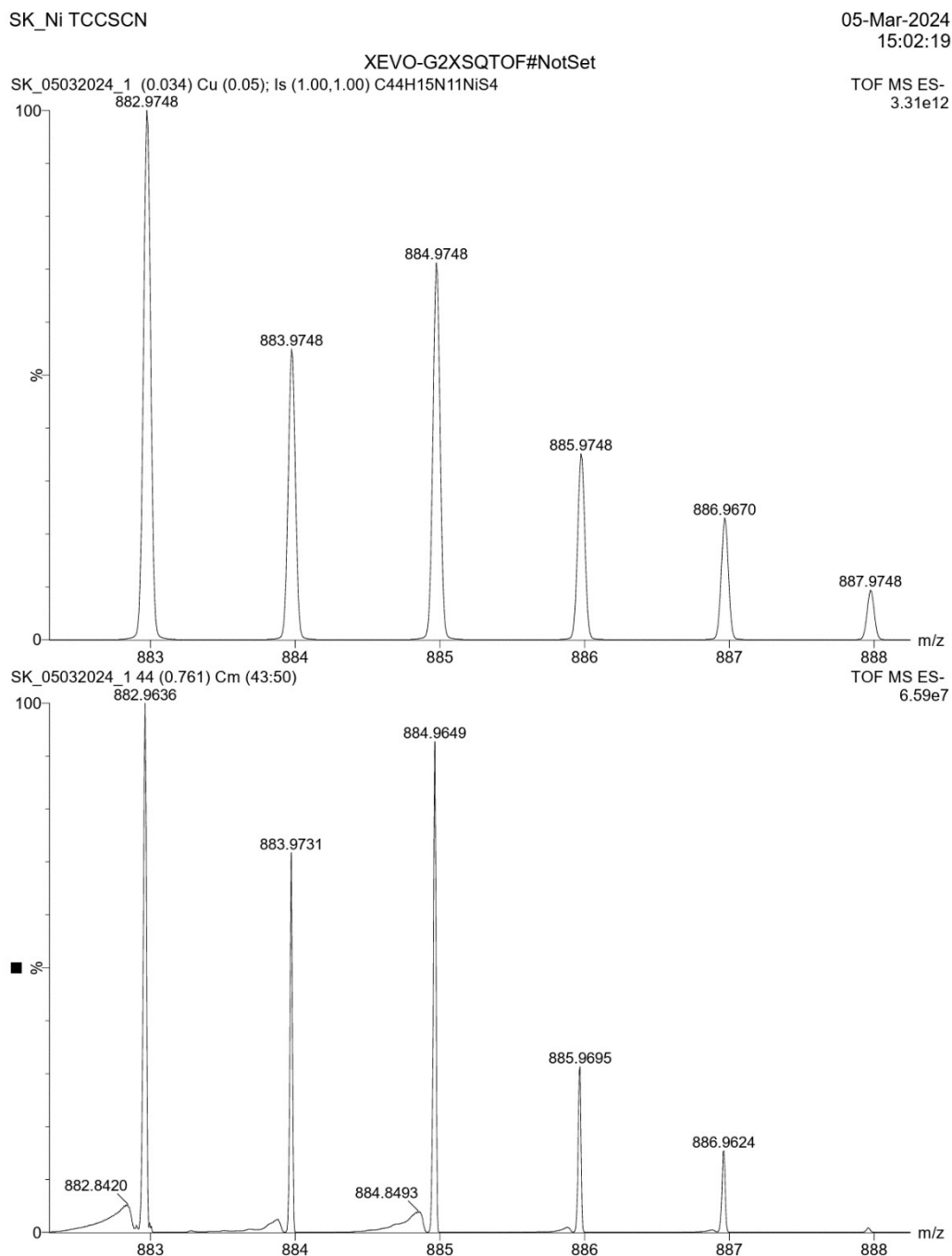


Fig. S5 (b) ESI-MS spectrum of 2,3,17,18-Tetrathiocyanato-[5,10,15-tris(4-cyanophenyl)corrolato] nickel(II), **1** in CH₃CN shows the isotopic distribution pattern (simulated).

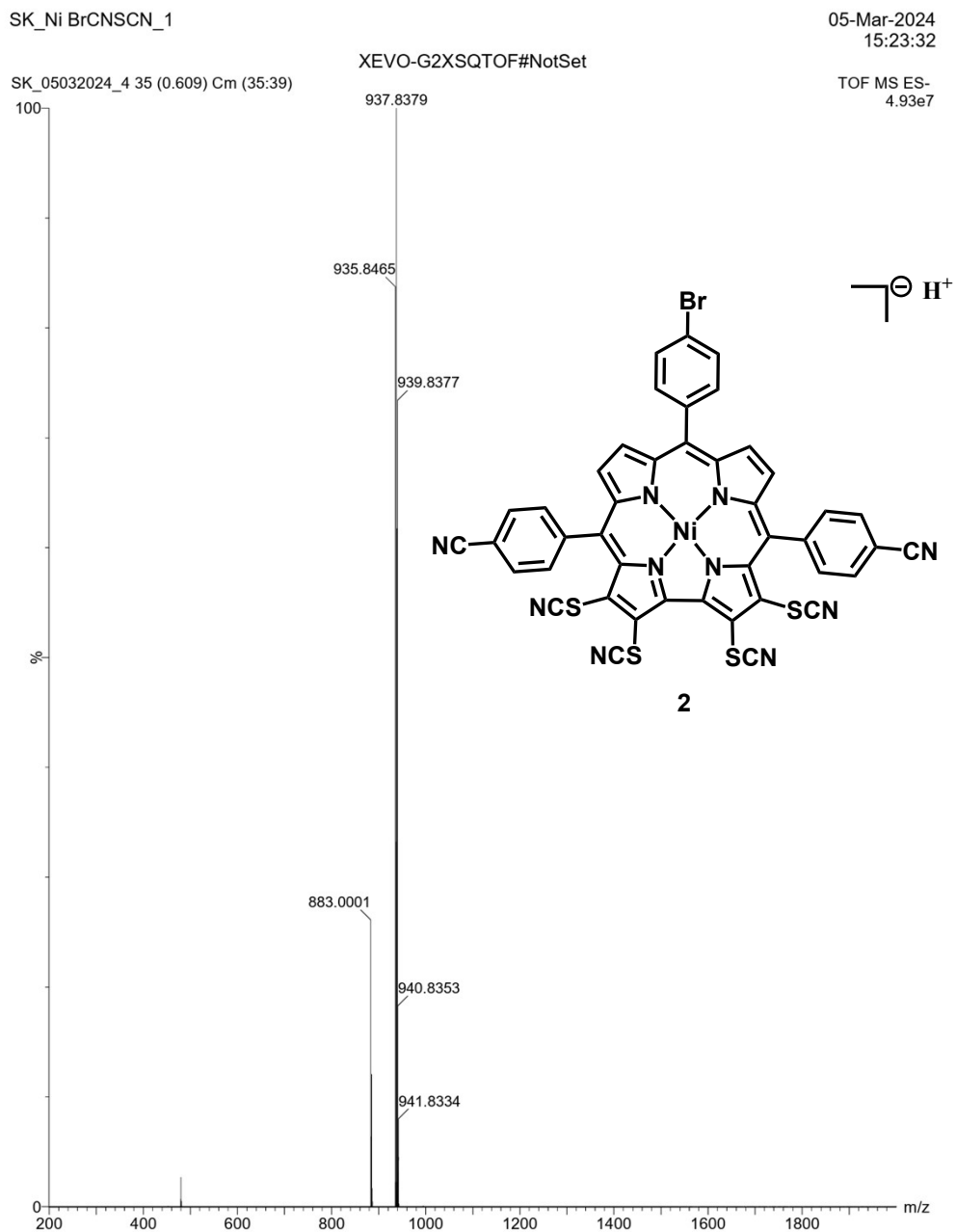


Fig. S6 (a) ESI-MS spectrum of 2,3,17,18-Tetrathiocyanato-[5,15-bis(4-cyanophenyl)-10-(4-bromophenyl)-corrolato] nickel(II), **2** in CH₃CN shows the measured spectrum (experimental).

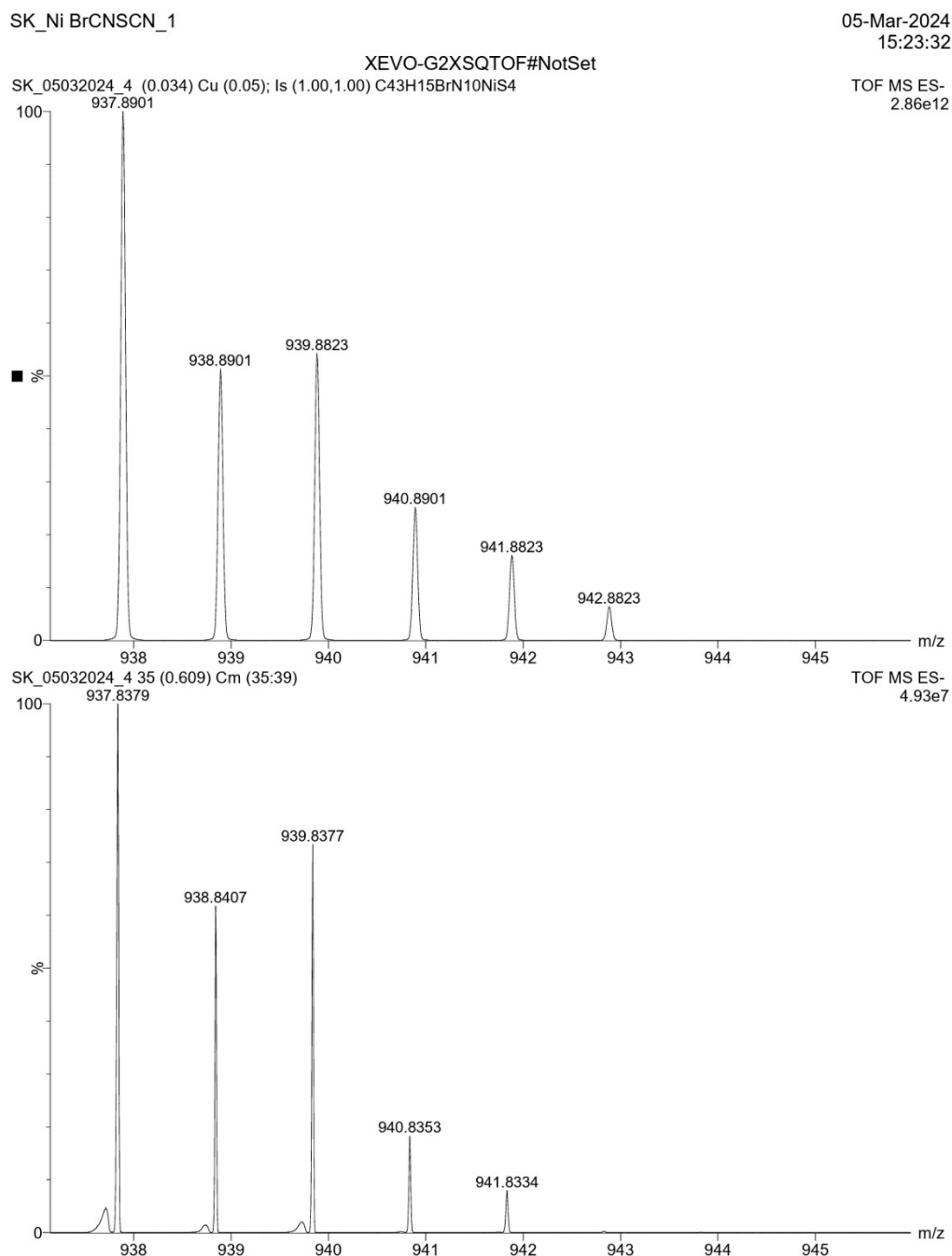


Fig. S6 (b) ESI-MS spectrum of 2,3,17,18-Tetrathiocyanato-[5,15-bis(4-cyanophenyl)-10-(4-bromophenyl)-corrolato] nickel(II), **2** in CH₃CN shows the isotopic distribution pattern (simulated).

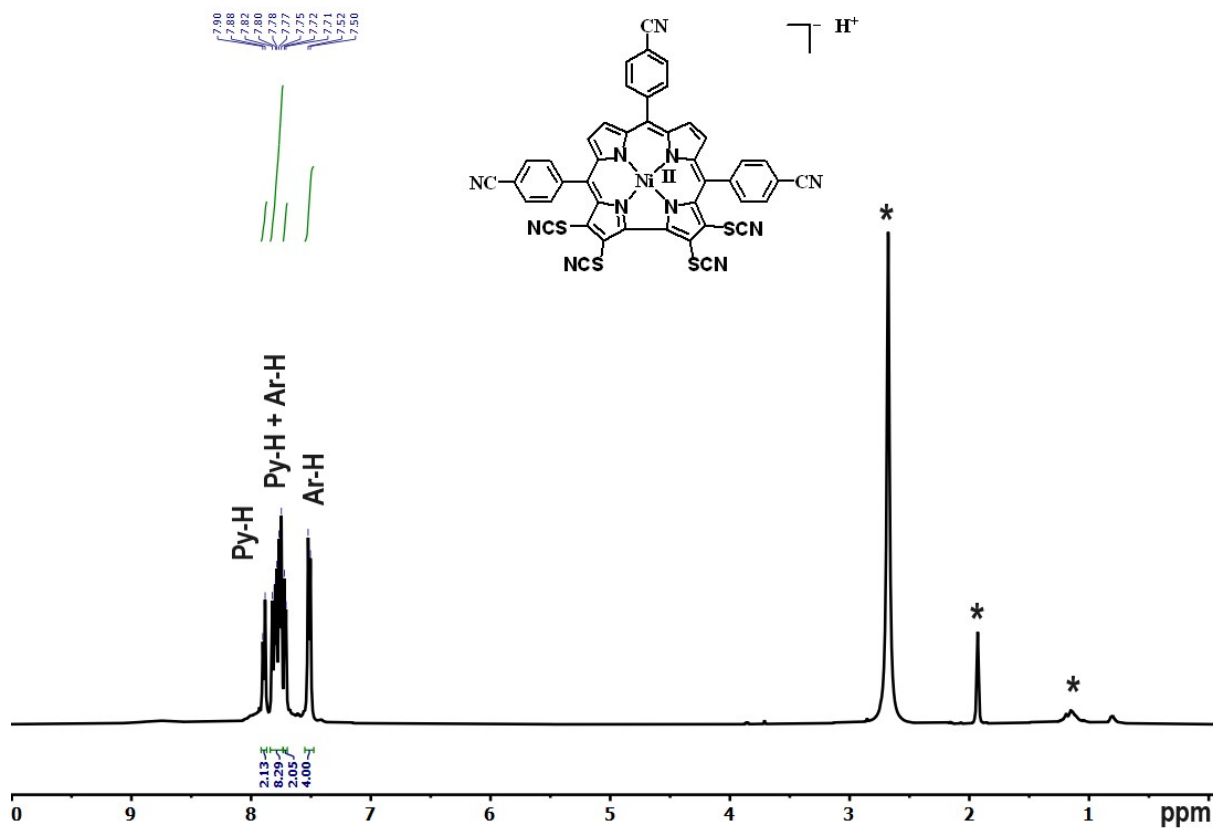


Fig. S7 ¹H-NMR spectrum of **1** in CD₃CN solution.

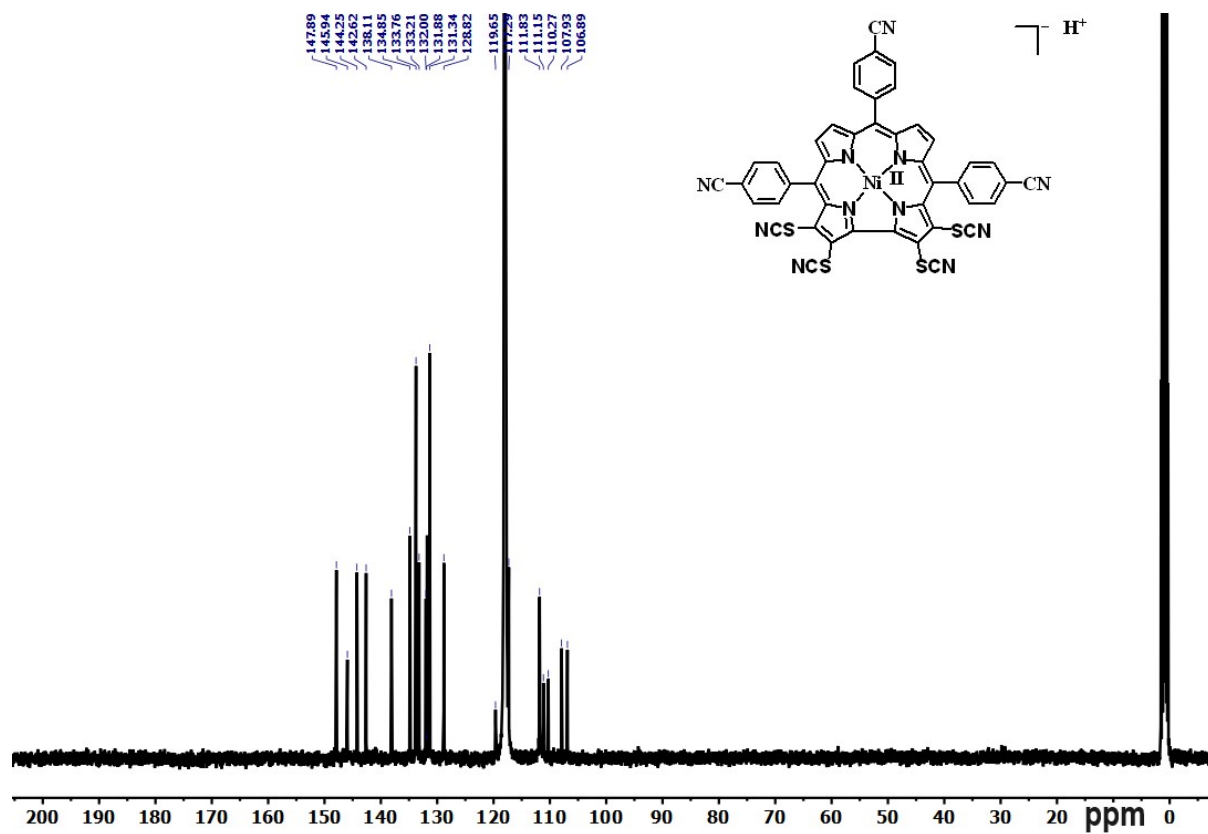


Fig. S8 ^{13}C $\{^1\text{H}\}$ -NMR spectrum of **1** in CD_3CN solution.

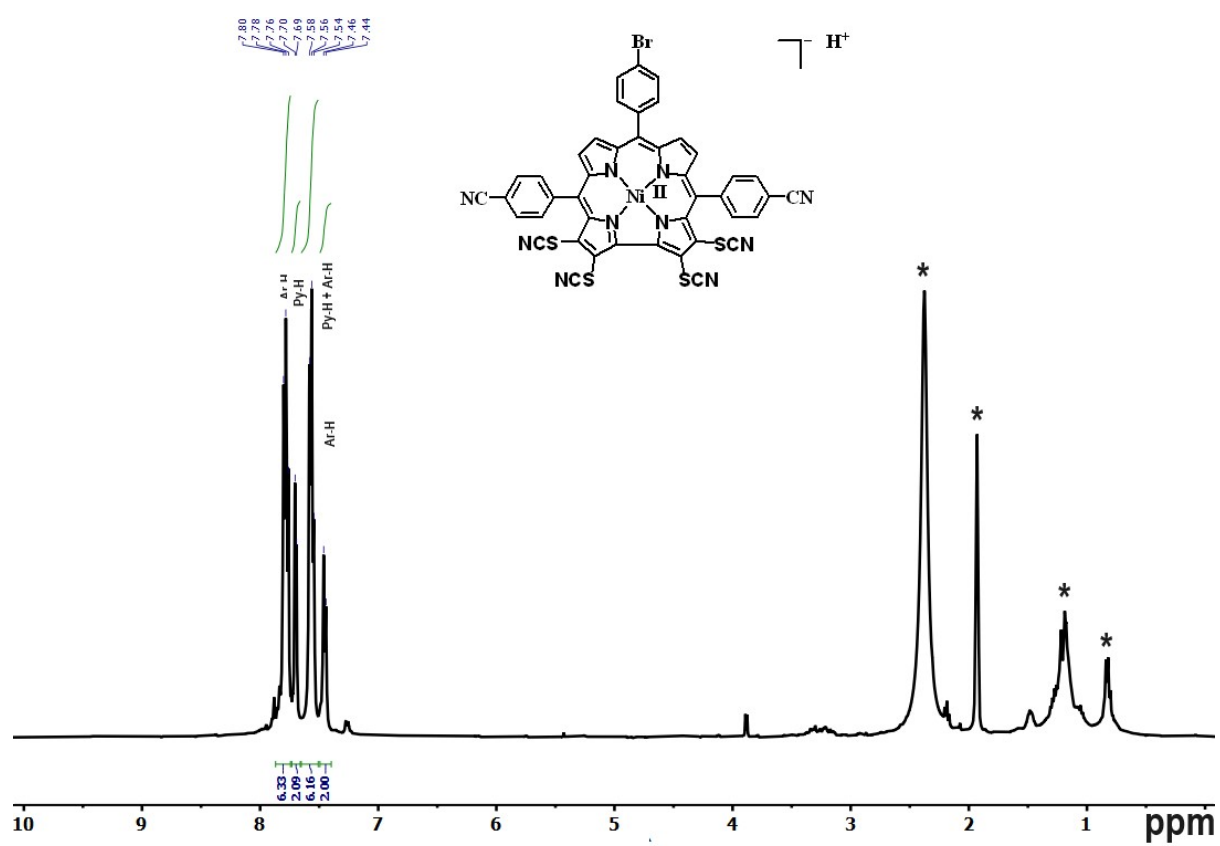


Fig. S9 ¹H-NMR spectrum of **2** in CD₃CN solution.

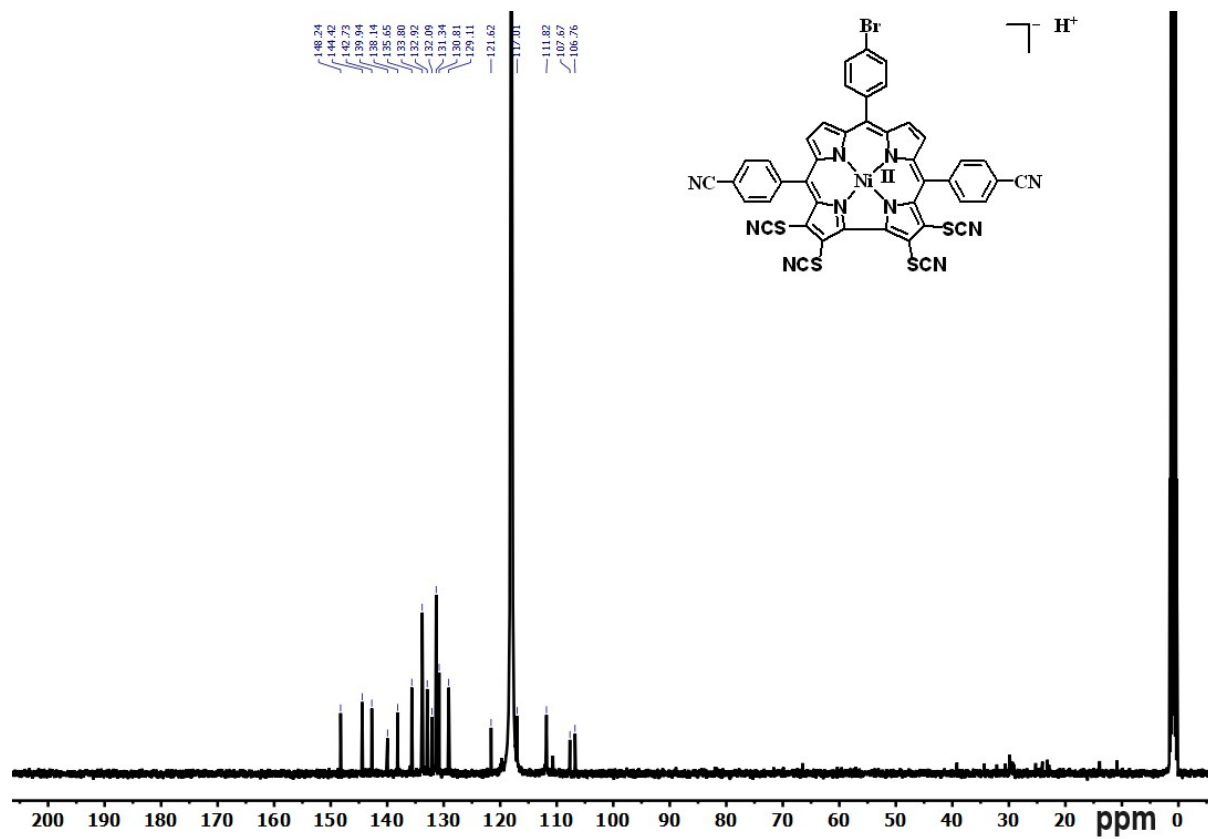


Fig. S10 ¹³C {¹H}-NMR spectrum of **2** in CD₃CN solution.

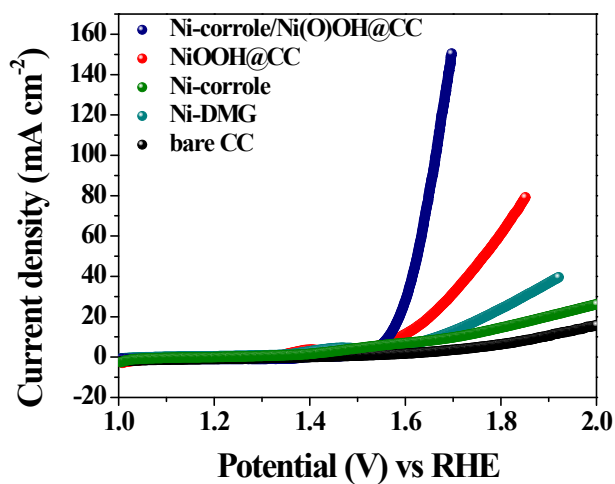


Fig. S11 LSV profiles of Ni(O)(OH)/Ni-corrole (active catalyst after 100 CV cycles), Ni(O)OH, Ni-corrole, and another molecular complex Ni(dmgh)₂ and bare CC in a 1.0 M aqueous KOH solution (scan rate 2 mV s⁻¹).

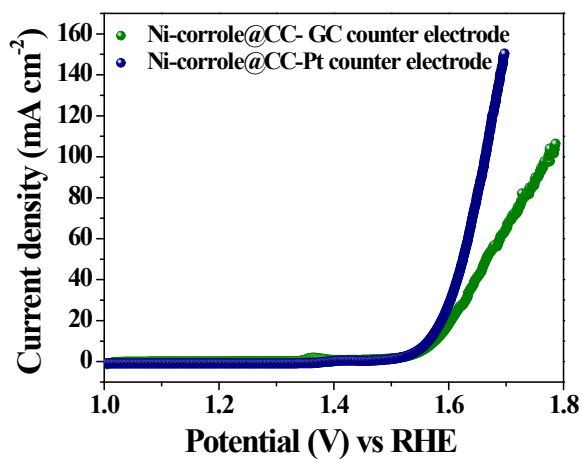


Fig. S12 LSV profiles of the Ni(O)(OH)/Ni-corrole@CC with Pt as counter electrode (blue) and Ni(O)(OH)/Ni-corrole@CC with respect to glassy carbon (green) as counter electrode in 1.0 M aqueous KOH solution.

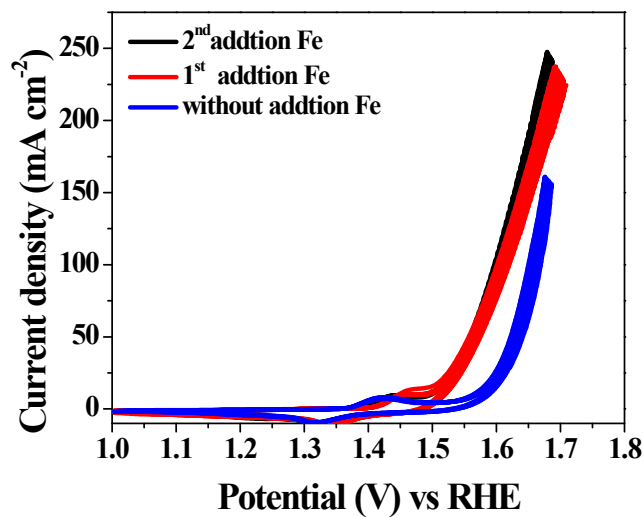


Fig. S13 Electrochemical activation of Ni(O)(OH)/Ni-corrrole via the addition of Fe³⁺ to the electrolyte solution, as depicted by a CV cycle.

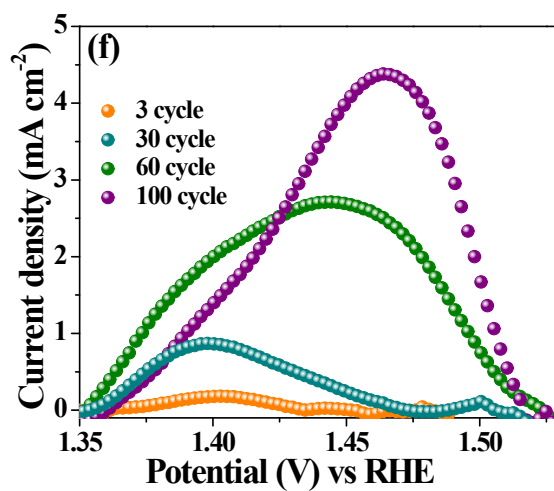


Fig. S14 Potential vs. current density plots showing the oxidation peak used for the area integration curve.

Appendix 3: Determination of the number of active sites of the Ni(O)(OH)/Ni-corrrole with respect to the different activation cycles.

Determination of the Number of Active Sites after 3 cycle activation ³

The area calculated (associated with the oxidation peak) = $0.0011 \times 10^{-3} \text{ V A}$

The associated charge calculated is = $0.0011 \times 10^{-3} \text{ V A} / 0.005 \text{ V s}^{-1} = 2.2 \times 10^{-3} \text{ A s} = 2.2 \times 10^{-4} \text{ C}$

Thus the number of electron transferred is = $2.2 \times 10^{-4} \text{ C} / 1.602 \times 10^{-19} \text{ C} = 1.37 \times 10^{15}$

Since the oxidation of Ni²⁺ to Ni³⁺ is a single electron transfer reaction, the number of electrons calculated above is the same as the number of active surface sites.

Hence, the surface-active site that participated in OER is = 1.37×10^{15} .

Determination of the Number of Active Sites after 30 cycle activation ³

The area calculated (associated with the oxidation peak) = $0.063 \times 10^{-3} \text{ V A}$

The associated charge calculated is = $0.063 \times 10^{-3} \text{ V A} / 0.005 \text{ V s}^{-1} = 12.6 \times 10^{-3} \text{ A s} = 12.6 \times 10^{-3} \text{ C}$

Thus the number of electron transferred is = $12.6 \times 10^{-3} \text{ C} / 1.602 \times 10^{-19} \text{ C} = 7.86 \times 10^{16}$

Since the oxidation of Ni²⁺ to Ni³⁺ is a single electron transfer reaction, the number of electrons calculated above is the same as the number of active surface sites.

Hence, the surface-active site that participated in OER is = 7.86×10^{16} .

Determination of the Number of Active Sites after 60 cycle activation ³

The area calculated (associated with the oxidation peak) = $0.309 \times 10^{-3} \text{ V A}$

The associated charge calculated is = $0.309 \times 10^{-3} \text{ V A} / 0.005 \text{ V s}^{-1} = 61.8 \times 10^{-3} \text{ A s} = 61.8 \times 10^{-3} \text{ C}$

Thus the number of electron transferred is = $61.8 \times 10^{-3} \text{ C} / 1.602 \times 10^{-19} \text{ C} = 38.57 \times 10^{16}$

Since the oxidation of Ni²⁺ to Ni³⁺ is a single electron transfer reaction, the number of electrons calculated above is the same as the number of active surface sites.

Hence, the surface-active site that participated in OER is = 38.57×10^{16}

Determination of the Number of Active Sites after 100 cycle activation ³

The area calculated (associated with the oxidation peak) = $0.381 \times 10^{-3} \text{ V A}$

The associated charge calculated is = $0.381 \times 10^{-3} \text{ V A} / 0.005 \text{ V s}^{-1} = 76.2 \times 10^{-3} \text{ C}$

Thus, the number of electron transferred is = $76.2 \times 10^{-3} \text{ C} / 1.602 \times 10^{-19} \text{ C} = 47.56 \times 10^{16}$

Since the oxidation of Ni²⁺ to Ni³⁺ is a single electron transfer reaction, the number of electrons calculated above is the same as the number of active surface sites.

Hence, the surface-active site that participated in OER is = 47.56×10^{16}

Calculation of TOF ⁴

$$\text{TOF} = (j \times N_A) / (4 \times F \times n)$$

Where,

j = Current density at 330 mV

N_A = Avogadro number

F = Faraday constant

n = Number of active Ni-sites

$$\begin{aligned} \text{TOF} &= [(10.12 \times 10^{-3}) (6.023 \times 10^{23})] / [(96485) (4) (47.565 \times 10^{16})] \\ &= 3.32 \times 10^{-2} \text{ s}^{-1} \end{aligned}$$

Table S3. Comparison of the number of active sites of the Ni(O)(OH)/Ni-corrole with respect to the different activation cycles.

S.No.	Active catalyst	Number active sites
1	Ni(O)(OH)/Ni-corrole (3 rd cycle)	1.37×10^{15}
2	Ni(O)(OH)/Ni-corrole (30 th cycle)	7.86×10^{16}
3	Ni(O)(OH)/Ni-corrole (60 th cycle)	38.57×10^{16}
4	Ni(O)(OH)/Ni-corrole (100 th cycle)	47.56 $\times 10^{16}$

Reference:

1. A. K. Singh, S. Ji, B. Singh, C. Das, H. Choi, P. W. Menezes and A. Indra, *Mater. Today Chem.* 2022, **23**, 100668.
2. S. Anantharaj, M. Jayachandran and S. Kundu, *Chem. Sci.*, 2016, **7**, 3188-3205.

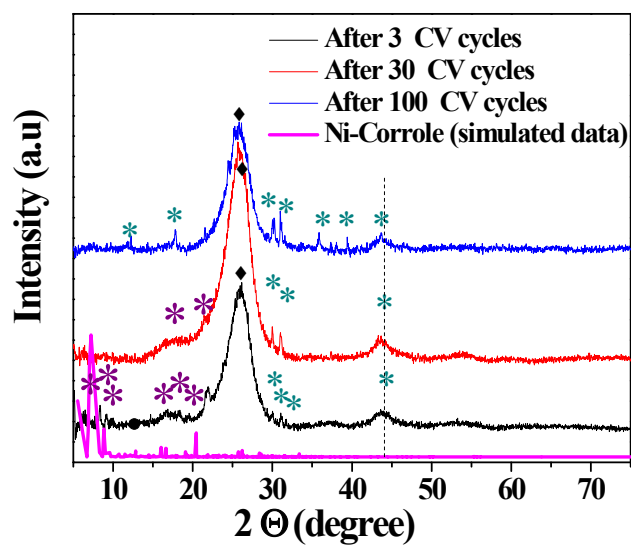


Fig. S15 PXRD of the Ni(O)(OH)/Ni-corrode after 3 CV cycles, 30 CV cycles, and 100 CV cycles.⁵ (Purple*: Ni-corrode complex, Cyan*: Ni(O)OH, ◆: Carbon cloth)

Reference:

3. Z. Lin, P. Bu, Y. Xiao, Q. Gao and P. Diao, *J. Mater. Chem. A*, 2022, **10**, 20847–20855.

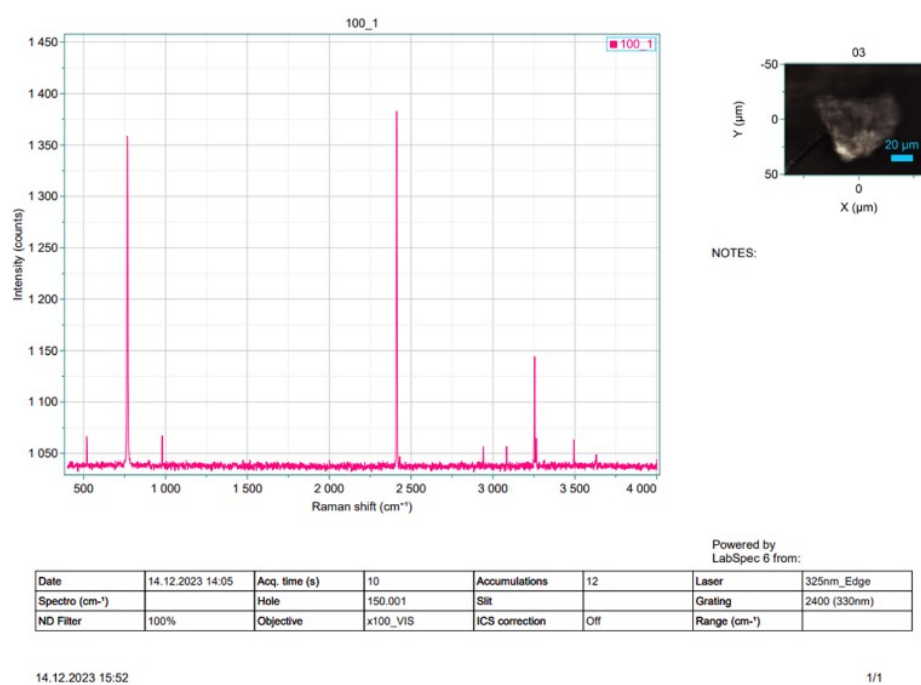


Fig. S16 Raman spectra of the Ni(O)(OH)/Ni-corrrole after 100 cycles.⁶

Reference:

4. K. M. Cole, D. W. Kirk and S. J. Thorpe, *J. Electrochem. Soc.* 2018, **165**, 3122.

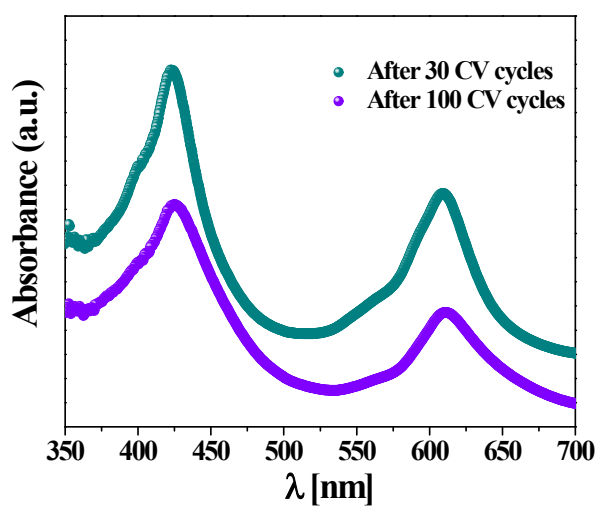


Fig. S17 UV-visible spectra showed the peaks corresponding to the Ni(O)(OH)/Ni-corrrole after 30 CV cycles and 100 CV cycles activation.⁷

Reference:

5. S. Eulberg, N. Schulze, J. Krumsieck, N. Klein and M. Bröring, *Angew. Chemie Int. Ed.* 2023, **62**, e202306598.

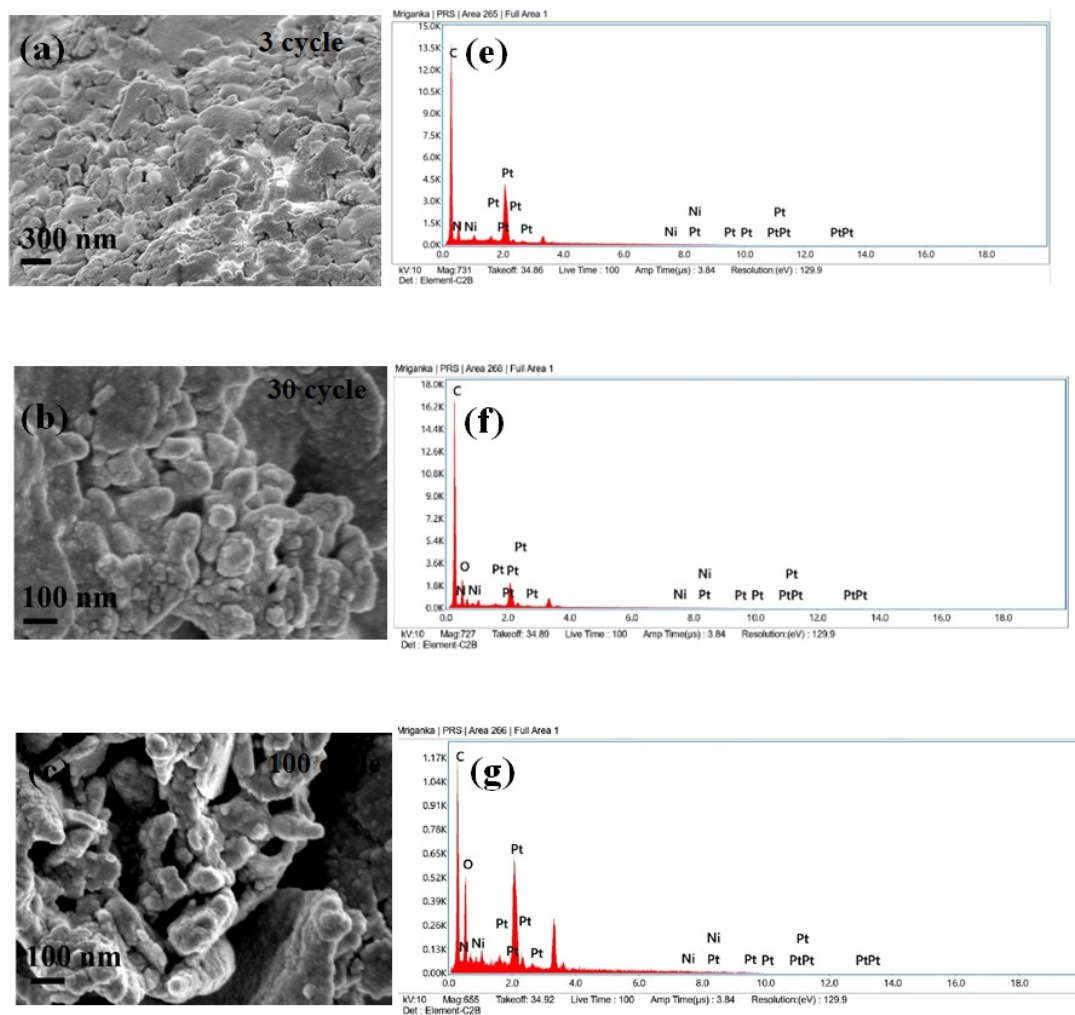


Fig. S18 (a-c) The SEM and EDX studies of Ni(O)(OH)/Ni-corrole after the different CV cycle-activation showed a change in the morphological feature. (e-g) The EDX data of the catalyst after 3 cycles, 30 cycles, and 100 cycles of CV activation showed that Ni, C, N, O, and S but with a varying amount.

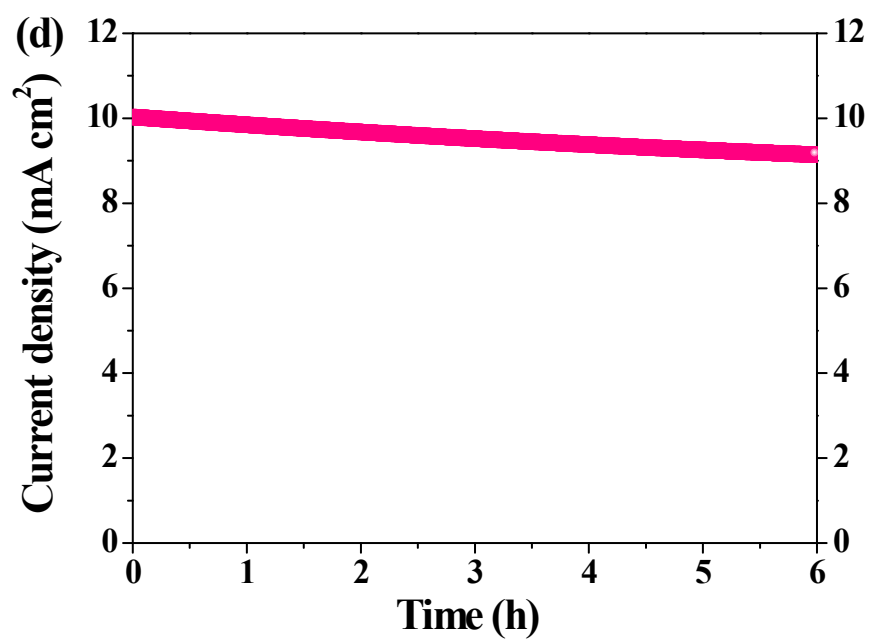


Fig. S19 The chronoamperometric study of Ni(O)(OH)/Ni-corrole demonstrates the stability of the catalyst for 6 hours.

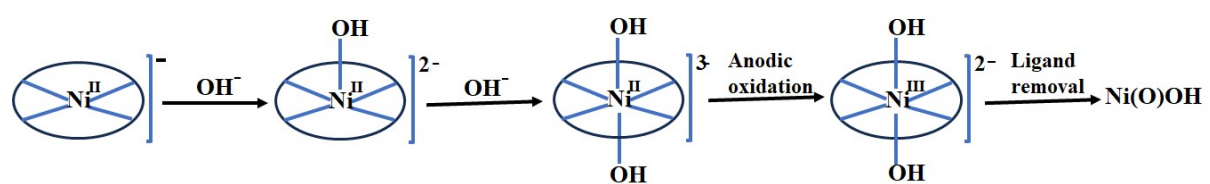


Fig. S20 The plausible mechanism for the formation of Ni(O)OH from the Ni-corrole complex by the anodic activation in the alkaline medium.